ORIGINAL PAPER

Changes of surface properties of sucrose particles during grinding in a cocoa butter-based suspension and their influence on the macroscopic behavior of the suspension

Knut Franke[1,2] · Ute Bindrich[2] · Sarah Schroeder[2] · Volker Heinz[2] · Dana Middendorf[2]

Abstract

Chocolate mass is a cocoa butter-based suspension, which mainly consists of sugar and cocoa particles dispersed in a continuous lipid phase. During chocolate manufacturing, sugar particles have to be ground to sizes below 25–30 μm. Such a fine grinding is carried out either by five roll refiners or by ball mills. Despite obtaining similar particle size distributions at the end, the grinding procedures result in different chocolate mass properties. The reasons for that are not fully understood, so far. Therefore, changes in particle sizes and surface properties of sucrose particles as well as their interactions with surrounding cocoa butter during the different grinding processes were investigated including atomic force microscopy techniques to characterize local surface states. It was found that especially the alteration of surfaces during continued grinding differed. In the case of roller grinding, surface states became more inhomogeneous and different surfaces states at microscopic level existed in parallel. More homogenous surfaces but with a higher degree of amorphous states were formed during grinding in the ball mill. Variations in macroscopic behavior of the suspension can be explained by the differences in interaction of particles with each other and with the surrounding lipid phase.

Keywords Sucrose grinding · Cocoa butter-based suspension · Surface properties · Amorphization · Atomic force microscopy AFM

Introduction

Molten plain chocolate, or chocolate mass, mainly consists of sugar and cocoa as the dispersed solid fraction and liquid cocoa butter as the continuous lipophilic phase [1]. While the cocoa fraction already possesses the required low particle size before added to the chocolate manufacturing process, sugar particles have to be ground to sizes below 25 to 30 μm to avoid a sandy mouthfeel [2, 3]. Therefore, sugar is the main component affected by a fine grinding, also mentioned as refining process during manufacturing of plain chocolate. For manufacturing of high-quality chocolates, mainly

5-roller refiners are used in central Europe together with a pre-roll refiner [2]. Besides roller grinding, fine grinding during chocolate manufacturing is performed using stirred media mills or ball mills, as well [2, 4].

Despite the limitations in maximum particle size, refining should result in a chocolate mass with low yield value and viscosity for a defined fat content [5]. Additionally to particle size distribution (PSD), surface properties of the particles are assumed to affect flow properties of chocolate masses due to their effect on interactions between the particles themselves as well as on interactions of particles and their surrounding liquid cocoa butter phase [6, 7].

It is well known that amorphous surfaces can be created due to the local mechanical energy input during breaking of the crystalline sucrose particles [8]. These amorphous surface areas play a distinct role in the distribution of flavor components and thus in chocolate sensory [9]. Gloria and Sievert [10] observed that all amorphous parts disappeared at the end of the grinding process. In contrast, Middendorf et al. [6] showed that the two fine grinding techniques resulted in different amorphous structures, which could be

✉ Knut Franke
franke@lw.uni-hannover.de

1 Present Address: Institute of Food Science and Human Nutrition, Leibniz University Hannover, Am Kleinen Felde 30, 30167 Hannover, Germany

2 DIL German Institute of Food Technologies, Prof.-Von-Klitzing-Straße 7, 49610 Quakenbrück, Germany

distinguished even after the grinding process had been finished. For this purpose, surfaces of the solid particles before and after grinding were characterized using atomic force microscopy (AFM) in combination with local thermal analysis (LTA). The different viscosities and yield values measured in such type of suspensions after ball or roller grinding could be attributed to different amorphous structures at the end of the grinding process.

However, it is still unknown, whether such surfaces are completely modified or whether there is a certain distribution of crystalline and amorphous regions on the surfaces at microscopic level and, finally yet importantly, how they change during the entire grinding progress.

Therefore, samples obtained during the different grinding processes were analyzed with respect to kinetic of moisture sorption behavior to characterize amorphous surface properties [11, 12], immobilized fat content, and resulting flow properties. These macroscopic data were combined with results from AFM applied to determine local amorphous and/or crystalline surface areas on microscopic level by measuring local softening temperatures using LTA.

Materials and methods

Sample material

In all experiments, the same lot of sucrose of EU quality II (Südzucker AG, Germany, kindly provided by Bühler AG, Uzwil, Switzerland) was used. Sucrose was stored at about 22 °C and 50% r.h. ensuring that potential amorphous regions are completely recrystallized [13]. Cocoa butter was kindly provided by August Storck KG Halle, Westfalen, Germany. Besides sucrose, fructose, maltose (Merck, Darmstadt, Germany), and anhydrous glucose (AppliChem, Darmstadt, Germany) were used for calibration of the AFM-LTA system.

Grinding procedures

Grinding in the ball mill (Wienerroto W-1-S, Wiener & Co., Amsterdam, Netherlands) was performed four times with 450 g sucrose and 550 g molten cocoa butter in one batch at 45 °C using steel balls with a diameter of 5 mm (10 kg) and with a diameter of 6 mm (10 kg) Agitation speed was 260 min^{-1}. Samples of each set were taken after different grinding times and included in the analyses.

An industrial scale 5-roller refiner of company Bühler AG (Uzwil, Switzerland) was used for roller grinding as described by Khajehesamedini et al. [14]. It was combined with a pre-refiner to reduce particle size of crystalline sucrose so that the mass can be transferred to the 5-roller refiner. Diameters and speeds of the rolls as well as roll gap

adjustment during grinding were the same as under industrial conditions [14]. The initial fat content of the suspension for roller grinding was set to 23 g/100 g suspension. During the roller grinding process, sampling was possible after the mass had been passed the gaps between the different rolls. Therefore, samples yielded from roll #2 after passing the gap between rolls #1 and #2, from roll #3 (after gap between #2 and #3), from roll #4 (after gap between #3 and #4) and from roll #5 after passing the last gap were available for analysis. Furthermore, samples were taken after the pre-refiner and from the crystalline sucrose before grinding. Grinding procedure at roller refiner was carried out three times with 20 kg mass per set.

Immediately after roller grinding, fat content of the suspensions was increased to 55 g/100 g (w/w) to obtain the same fat content as in the suspension ground in the ball mill. For this purpose, the required amount of liquid cocoa butter was added to the ground mix. This blend was mixed at a temperature of 50 °C using a laboratory mixer (RW 20 DZM, Janke + Kunkel, IKA-Werk, Germany) with a speed of 300 rpm for 30 min. Homogeneity of the blend was checked visually with respect to the absence of solid agglomerates.

Grinding parameters for the roller refiner and the ball mill were chosen according to standard conditions in the chocolate industry and not varied. Ball mill grinding time was adapted to be consistent to the particle sizes obtained after roller grinding.

Determination of PSD

A laser diffraction spectrometer Mastersizer 2000 with dispersion unit Hydro 2000S (Malvern Instruments Ltd., Worcestershire, UK) was used to measure the PSD of the sucrose particles in the suspension according to ISO 13320-1. Mineral oil (Shell Oil S. 4919, Shell GmbH, Hamburg, Germany) was applied as dispersion medium. PSD was described by the volume distribution and the specific particle surface area (SPSA) was calculated using the device software. The SPSA represents the sum of the surface areas of all particles related to the mass of all particles in the suspension. Each volume distribution is a result of more than 10 single measurements, which are automatically averaged by the instrument software. Obscuration during measurement was kept at 50% ± 10%, stating that particle concentrations were comparable for all determinations.

Sample preparation for individual sucrose particles

To obtain the individual ground sucrose particles, 250 g of the suspension were centrifuged in a Biofuge primo (Heraeus, Germany) at 45 °C and 5100 g for 10 min. A glove box was used for further processing of the samples after centrifugation to avoid access of the solid surfaces to moisture from

air. This glovebox is a completely sealed box with integrated rubber gloves to handle the material inside in an atmosphere of dried nitrogen. Moisture in the gas was reduced using silica gel and controlled by a hygrometer.

The supernatant cocoa butter was decanted and cocoa butter residues on solids were washed off using n-hexane (A.R.TM 95%, LabScan, Gliwice, Poland). Afterwards, single sucrose particles were glued onto freshly cleaved mica discs (V3 quality, preparation kit G3350A, Plano GmbH, Wetzlar, Germany). As demonstrated earlier, this sample preparation does not influence relevant surface properties of the sucrose particles [15].

Sorption properties

Defatted and solvent free sucrose particles (2–3 g) were weighed in borosilicate glass cups (46 mm Ø) at the dry environment (r.h. < 10%) of the glove box and the glass cups were sealed with parafilm afterwards. A precision balance AT 460 (Mettler Toledo Giessen, Germany) inside the glove box connected with a computer was used to follow the mass changes with three measurements per second. Constant environmental conditions for sorption experiments in the glove box were 24 °C and 64% r.h. The glass cups were positioned on the balance and measurement procedure started after the parafilm was perforated by contactless overheating. Absolute and relative, as related to the initial mass, changes in sample mass were calculated. The sorption behavior was described by the initial slope of the relative mass change in percent per min observed at the beginning of the storage at the humid conditions mentioned above. The steeper this initial mass increase is, the more hygroscopic is the particle surface. This measurement was carried out in triplicate for each grinding step.

Determination of adhesion forces and state of sucrose particle surfaces by AFM

An MFP 3D™ AFM (SA, Asylum Research, Santa Barbara, USA) together with a standard silicon tip (OMCL-AC-240TS-E3, Olympus Corporation, Tokyo, Japan) was applied under controlled atmosphere (r.h. < 10%, 22 °C) for determination of adhesion forces. At least 15 particles per suspension were characterized and the results were merged to obtain the final force distributions. 30×30 force-versus-distance-curves per force map on a surface of 4 µm2 were measured in contact mode and adhesion forces were calculated. Eigenfrequency, quality factor, stiffness of the cantilever oscillation and cantilever's spring constant were determined from thermal noise by an analysis of the power spectral density of displacement fluctuations for each cantilever [16]. Contact trigger point was 1 V and scan velocity was 2 mm/s. Histograms of force maps were calculated

based on 100 force classes. Forces classes containing less than 0.5% of total numbers of measurement points were neglected. Data analysis was performed using IGOR Pro Software and Microsoft Excel®. To compare adhesion forces, mean value, variance, and excess of the individual histograms of the adhesion forces on the particles were calculated [17]. Parameters obtained from the individual histograms were averaged and the standard deviation of the parameters mentioned above was calculated.

LTA was used to measure softening temperatures [18] and was carried out with an AN2-200 ThermaLever in an atmosphere of dried nitrogen (voltage ramp 1 V/s, trigger 10 nm, set point 500 mV). Previous heating cycles were performed for tip cleaning before each measurement cycle. Standard deviation for all measurements was determined from the standard deviation of the resistance determined during sugar standard measurements and resulted to 7 K. Results were analyzed and amorphous regions were correlated with a temperature range of 50–90 °C, a mixed surface state to a range of 90–155 °C and a crystalline surface state to 155–220 °C [6, 19, 20]. The resulting diagrams show the share of measurement points for a certain softening temperature range related to the total number of analyzed measurement points, which was at least 75 points per grinding step.

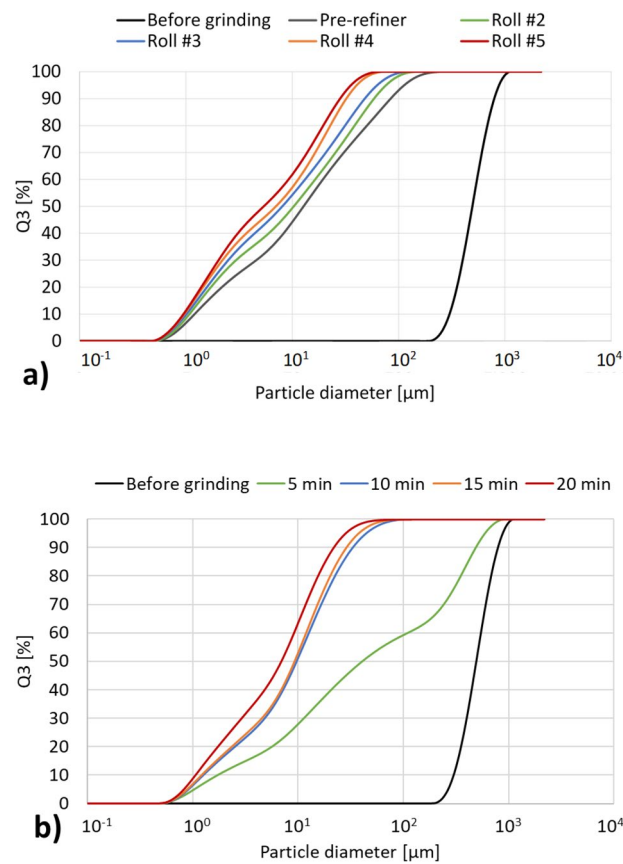## Fat immobilization and flow properties of the suspension

The amount of immobilized fat can be determined by centrifugation of the suspension followed by a quantification of the amount of supernatant [11, 21]. For this purpose, 15 ± 0.01 g suspension heated to 45 °C were centrifuged for 10 min at 5100 g (RC-5, Sorvall, Bad Nauheim, Germany). The supernatant was decanted and weighed. Based on this amount of removable or non-immobilized fat, the amount of immobilized fat in g fat per g sucrose was calculated considering the total fat content of the suspension and it was related to the SPSA obtained from the PSD (The section "Adhesion properties of particle surfaces") to calculate the surface area-related fat immobilization. Measurements were carried out in triplicate.

Flow properties of the suspension were determined at 40 °C using a rheometer (AR 2000, TA Instruments, New Castle, DE; USA) in the strain-controlled mode with concentric cylinders. Inner and outer diameters were 28 mm and 30 mm, respectively, and bob height was 42 mm. Sample preparation and measuring temperature were according to the IOCCC Method 46–2000 [22]. However, a broader shear rate range from 0.1 to 200 s^{-1} was applied including a pre-shearing at 20 s^{-1}. Measuring cycle itself started with a ramp with logarithmically increasing shear rates from 0.1 to 200 s^{-1} followed by a downward ramp back to 0.1 s^{-1}. Data of the downward ramp were used to calculate

the rheological parameters equilibrium viscosity and yield value according to a simplified rheological model proposed for molten chocolate mass by Tscheuschner [23] as shown in the equation below

$$\tau = \tau_0 + \eta_\infty \cdot \dot{\gamma} + \eta_{str} \cdot \dot{\gamma}^{1-n} \tag{1}$$

with τ as shear stress, τ_0 as yield value, η_∞ as equilibrium viscosity, $\dot{\gamma}$ as shear rate, η_{str} as structure-depended viscosity, and n as flow index. Measurements of the flow curves were performed in triplicate.

Fig. 1 Cumulative volume distribution of the sucrose particle sizes before and after different grinding steps during **a** roller grinding and **b** ball mill grinding

Results and discussion

Particle size distribution (PSD)

The initial PSD of the crystalline sucrose as well as the PSD after the different grinding steps and processes are summarized in Fig. 1 as cumulative volume distributions. Figure 1a shows the PSD after roller grinding and Fig. 1b those after ball mill grinding. The distribution parameters are listed in Tables 1 and 2, respectively.

Both grinding techniques sufficiently reduce the sizes of the sucrose particles with respect to the production of high-quality chocolate as indicated by the shift of the distribution curves to the left-hand side. It becomes also very clear that the main reduction in particle size can be attributed to the beginning of the grinding process, e.g., after roller #2 or after a short grinding time in the ball mill. This agrees with typical size reduction kinetics [14, 24]. However, the shift from this intermediate PSD to the final size distribution is less pronounced but does substantially contribute to reach the desired maximum particle size and the favorable PSD required to comply with the sensory demands [25].

After passing all gaps of the roller refiner, $\times 50$ and $\times 10$ of the PSD are similar whereas $\times 90$ after roller grinding was slightly higher (cf. Table 1). Similar results were reported in previous studies [5, 6].

Water sorption properties of sucrose particles

Because the particle size is continuously reduced, lots of new surfaces are generated during grinding. It is already known that the mechanical impact on the particles during grinding is connected to changes from crystalline to

Table 2 Cumulative volume distribution parameters of the sucrose particles before and after different grinding steps during ball milling

	Before grinding	5 min	10 min	15 min	20 min
$\times 10$	228 ± 40	1.73 ± 0.02	1.26 ± 0.05	1.22 ± 0.01	1.06 ± 0.03
$\times 50$	490 ± 4	40.9 ± 0.8	9.70 ± 0.11	9.26 ± 0.13	6.95 ± 0.03
$\times 90$	847 ± 28	489 ± 2	33.0 ± 0.9	28.7 ± 0.1	23.0 ± 0.5
Span	1.27	11.91	3.27	2.97	2.99

Table 1 Cumulative volume distribution parameters of the sucrose particles before and after different grinding steps during roller refining

	Before grinding	Pre-refiner	Roll #2	Roll#3	Roll #4	Roll #5
$\times 10$	228 ± 40	1.20 ± 0.03	1.08 ± 0.01	1.01 ± 0.01	0.96 ± 0.01	0.94 ± 0.01
$\times 50$	490 ± 4	12.5 ± 0.1	10.3 ± 0.1	8.04 ± 0.05	6.99 ± 0.06	5.38 ± 0.01
$\times 90$	847 ± 28	84.1 ± 9.3	58.6 ± 0.1	48.0 ± 0.2	32.1 ± 0.5	28.1 ± 0.2
Span	1.27	6.51	5.59	5.84	4.46	5.05

amorphous surface states. Water sorption properties, which can be described by the relative mass change during storage at ambient humidity and at temperature conditions where a re-crystallization of amorphous parts is expected, can deliver an indication about the bulk properties of the particle's surface state as mentioned before. In this study, we used the initial slope of the increase in relative mass change directly after exposing the sucrose surfaces to the humid ambient, because this parameter of the sorption behavior was best suited to characterize differences in sorption behavior. Other possible parameters for moisture adsorption behavior like equilibrium moisture content were difficult to reach and their determination would be too time consuming.

The results of the sorption measurements as the initial slope in mass increase of the particles are shown in Fig. 2a and b. As can be observed from the data in both diagrams, grinding in the ball mill resulted in steeper slopes of water sorption compared to roller grinding. This indicates that the particles after this type of grinding were more hygroscopic than the particles ground in the roller refiner. At the beginning of the grinding process, after pre-refiner or after the first 5 min in the ball mill, the sorption properties are quite similar. During progressing grinding, differences in

Fig. 2 Initial slope of the relative mass change during water vapor sorption of sucrose particles after different grinding steps during **a** roller grinding and **b** ball mill grinding

sucrose's hygroscopicity ground by either roller of ball mill slightly increased.

The first finding confirms that amorphous surfaces possessing a high hygroscopicity were generated due to the mechanical impacts in both types of grinding. An explanation for the lower degree of hygroscopicity after roller grinding might be related to a denser structure of the amorphous parts in the sucrose particles. They were formed during grinding between the rollers due to the relatively long impact of pressure and shear compared to grinding in a ball mill. Such dense parts can be expected to have a poorer accessibility for water molecules. Therefore, adsorption of water in these structures takes more time leading to smaller initial slopes.

Adhesion properties of particle surfaces

Despite the conclusive results obtained from the sorption measurements, this method is not able to reveal any information about surface area properties on microscopic scale, e.g. distribution of different surfaces states or their interaction with the local environment.

Therefore, histograms of AFM adhesion forces were used to characterize local surface areas after grinding as previously performed by Middendorf et al. [6]. The results are summarized in Fig. 3.

The mean value of the surface adhesion forces during roller grinding (Fig. 3a) is highest in the beginning of the grinding process after passing the first gap of the 5-roller refiner (roll #2) and decreases after passing the following gaps (rolls #3 to #5). Due to the pulses acting on the particle during grinding, the former highly ordered crystalline structure becomes unstructured, meaning that parts of the surface are amorphized. Therefore, the forces acting between the surface and the AFM probe increased in these parts due to larger contact areas. In parallel, due to a more inhomogeneous surface consisting of both amorphous and crystalline parts, deviation of local forces is increased, too. This is represented by the higher variance of the distribution (Fig. 3b), as this parameter describes the uniformity of adhesion forces measured on the surface and can be regarded as a measure of how much crystalline and amorphous surfaces are mixed. The lower the variance is, the more uniform the particle surface is. Accordingly, a low variance at the beginning of the roller grinding process (after roll #2) can be observed, which increases during the following grinding steps. A uniform particle surface with high adhesion forces means that large areas of the particle surface are in the amorphous state or at least showing a surface state where the upper molecular layers of sucrose molecules are not in the highly ordered crystalline state anymore.

During the continuing grinding process (rolls #3 to #5), the change in particle size per gap passage is lower (cf.
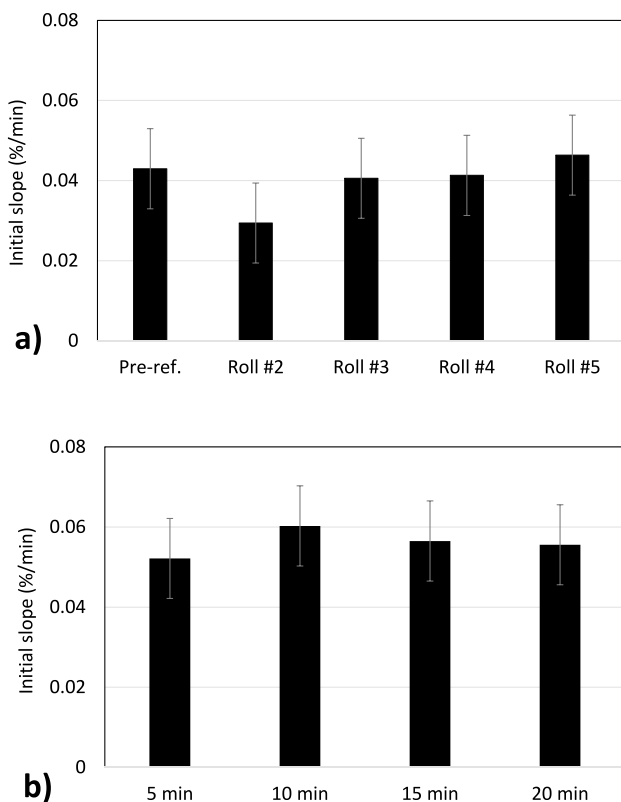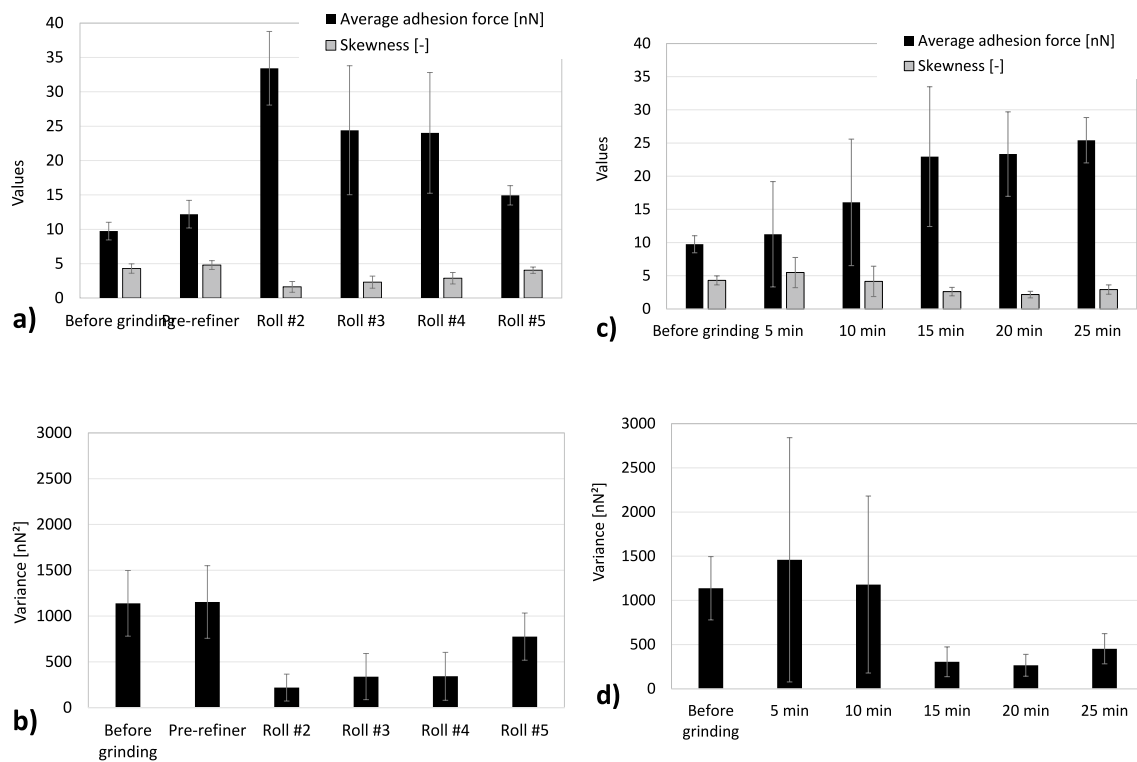
Fig. 3 Development of surface adhesiveness distribution parameter average value and skewness (**a** and **c**) as well as variance (**b** and **d**) during grinding by roller refiner (**a** and **b**) and during grinding in a ball mill (**c** and d)

Fig. 1). This indicates that less new surfaces are formed during each passage. The slight decrease in the average values indicates that adhesiveness became lower, whereas the variance increased. From the molecular point of view, it can be stated that the surface became less uniform indicating that structured and more or less unstructured surfaces existed together on particle surfaces. This trend continued during the following grinding steps showing a rising variability of surface states. Furthermore, the parallel increase in the skewness parameter of the adhesion force distributions supports this finding indicating a higher degree of non-uniformity of the adhesion forces with a broader range of single forces above the average force (positive skewness).

A different picture is obtained after evaluating these parameters for the ball mill grinding process (Fig. 3c and d). In this case, a slight increase in the average value for the adhesion force can be observed. This indicates not only that the newly generated surfaces are in the amorphous state, but also that this surface state is very stable. In addition, this assumption is supported by the fact that the variance at the end of the grinding process (Fig. 3d, 15 and 20 min) is much smaller compared to the first part of the grinding process (5 and 10 min). This means that the longer the grinding time was, the more breakage events occurred, and the more amorphous parts were generated. Therefore, less remaining crystalline parts are present because recrystallization is

prevented. Compared to the grinding process in the roller refiner, less particles are affected at the same time. Therefore, the average value of adhesion forces at the beginning is low, whereas the variance is higher, because amorphous surfaces are much broader distributed among the particles. During the grinding progress, an increasing portion of particles is impacted. This results not only in an increase of amorphous particle surfaces, but also in a more uniform distribution of these surface states, which is indicated by a decrease in variance of adhesive force distribution.

## Local thermal analysis of surface states

Softening temperatures can be attributed to the beginning of e.g. melting of the sucrose crystals or reaching glass transition temperatures of amorphous structures. The portions of each state on the total number of tested points in the classes are shown in Fig. 4. For roller grinding, a huge increase in the extent of amorphous surfaces was detected after the passage of the first roller gap (roll #2). However, after the last passage (roll #5) the portion of amorphous surface regions decreased (Fig. 4a). Additionally, a certain number of points with a mixed surface state was detected. These structures have already been described by Middendorf et al. [6]. They found that the surface state of sucrose particles after roller grinding is
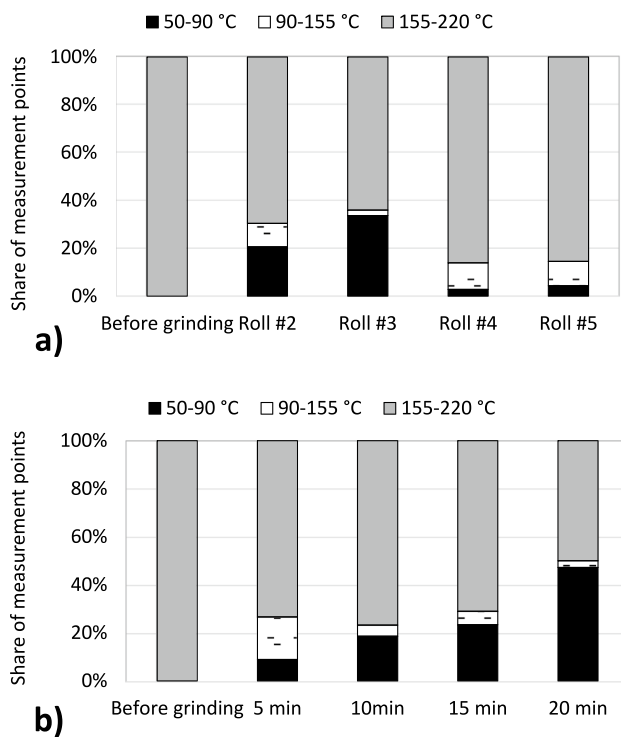
Fig. 4 Results of the AFM-LTA measurement of softening temperatures at sucrose particle surfaces before and after different grinding steps during **a** roller grinding and **b** ball mill grinding

predominantly characterized by such mixed surface states. A very different behavior was found for grinding in a ball mill (Fig. 4b) where a steady increase in the portion of amorphous surfaces with grinding time was found. These results are in good agreement with the results obtained from evaluation of adhesion force measurements.
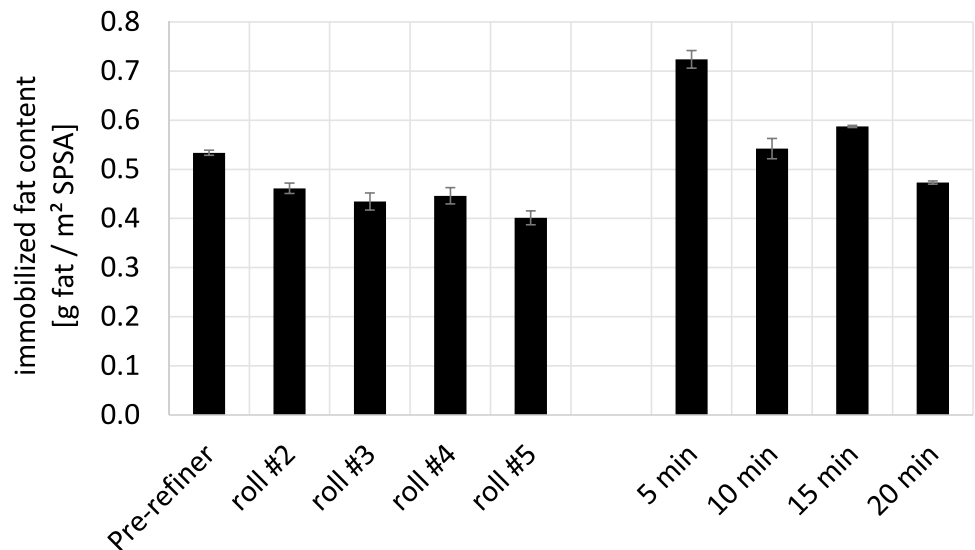
Immobilized fat content and flow behavior of the suspensions

It has to be mentioned that the amount of immobilized fat, which cannot be separated from the suspension by centrifugation did not only depend on fat immobilization on particle surfaces but it was also influenced by capillary effects in the tightly packed sediment. Since all measurements were carried out in the same way, the data obtained from these measurements should enable a comparison of the interactions between particle surfaces and fat phase [11]. Especially, a higher amount of immobilized fat is closely related to a higher viscosity of the suspension [7].

Middendorf et al. [6] already found that immobilized fat content on the surface of sucrose particles after grinding is lower for roller grinding compared to ball mill grinding. This finding is supported by the results of this study. Additionally, there are also distinct differences in the amount of immobilized fat after different grinding steps or times, respectively (Fig. 5).

As already described, the particle surface became less uniform after roller grinding, which was described as a mixed state and cannot be differentiated or described in detail, yet. A different picture is obtained after ball mill grinding. As described above, number of highly stable amorphous parts increased with grinding time and a more uniform distribution of amorphous areas was formed. It can be expected that this uniform distribution of amorphous areas possessed a high affinity to the surrounding fat phase resulting in a higher degree of fat immobilization.

The flow behavior of the suspensions changed due to the progressing degree of particle destruction during grinding. New surfaces are created within the suspension leading to an increasing number of contacts between the particles, which can strengthen internal structures related to resistance

Fig. 5 Immobilized fat content after roller (left) and ball mill grinding (right) calculated in g fat per square meter specific particle surface area (SPSA)

against shear [5, 7]. Therefore, the flow property parameters measured after each grinding step or time were related to the SPSA obtained from the PSD as represented in Fig. 6 to distinguish between the effects of increasing total surface area in the suspension and differences in surface properties of the particles.

As mentioned in the method section, flow curves of the chocolate masses were fitted with the rheological model according to Tscheuschner (Eq. 1). This model gave a very good fit over the whole shear rate range from 0.1 to 200 s^{-1} as indicated by the R2 values between 0.9965 and 0.9992. From this model, yield value τ_0 and equilibrium viscosity η_∞ were used below to discuss the flow behavior, because these parameters can be easily related to material properties of the molten chocolate and they describe most of the flow characteristics of molten chocolate mass. The other two parameters, structure-dependent viscosity η_{str} and flow index n, were not considered in the discussion below, because they are more like fitting parameters and they cannot be directly related to physical material properties.

Both yield value and equilibrium viscosity calculated with this model showed a dependency on SPSA. The higher the SPSA, the higher was the relevant parameter.

a)

b)
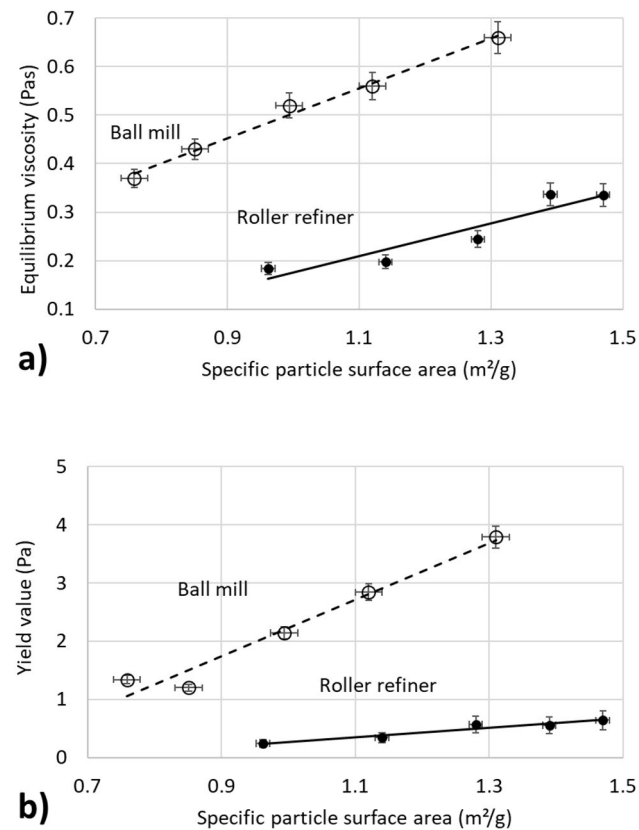
Fig. 6 Equilibrium viscosity a) and yield value b) of the cocoa butter-sucrose-suspensions versus the specific particle surface area (SPSA) of the sugar particles for the different grinding procedures

This confirms the assumptions given above and agrees with previous work [26, 27]. However, there were differences between the milling techniques. At similar SPSA, equilibrium viscosities of the suspensions ground in the roller refiner were much lower compared to those after grinding in a ball mill (Fig. 6a). This difference can be considered as a very strong indication that not only the amount of surface area but also the interactions between particle surface and surrounding fat environment influence the flow behavior. The equilibrium viscosity characterizes the flow behavior at very high shear rates where structures between particles are more or less disintegrated. Therefore, the influence of particle–particle-interactions is negligible under these conditions and only the hydrodynamic resistance of the single particles in the flow is of relevance [7]. Considering this, a higher viscosity indicates a stronger interaction of the particle surface with the surrounding fat, because more fat is immobilized on the surfaces increasing the hydrodynamic cross-sectional area. Comparing this behavior with the data from adhesivity measurements (Fig. 3), it seems that the decreasing average adhesion forces during progressing roller grinding results in a less strong interaction with the surrounding cocoa butter enabling lower equilibrium viscosities. Vice versa, the increasing adhesion forces measured on particle surfaces during grinding in a ball mill seemed to immobilize more fat around the particles leading to higher viscosity at the higher shear rates. The effect increased with smaller particles, because a higher amount of surface area for immobilizing the fat is available. This explanation is confirmed by the results for immobilized fat content (Fig. 5), since grinding in the ball mill gave a higher amount of immobilized fat related to the particle surface area compared to grinding in the roller mill.

Similar to the equilibrium viscosity, yield values were also lower after roller grinding compared to ball mill grinding at the same SPSA (Fig. 6b). The flow parameter yield value is related to particle–particle interaction before shearing or at very low shear rates where internal structures between particles still exists [7, 28]. It can be assumed that particle–particle-interactions are also determined by the particle's surface properties. The higher adhesion forces measured at the surfaces of the particles after a longer grinding in the ball mill seemed to enforce the interactions between particles, too, leading to stronger networks in the non-sheared suspensions as indicated by the higher yield value to overcome these structures. Overall, the results with respect to flow behavior indicate that higher adhesive forces measured on particle surfaces during grinding lead to stronger particle-to-particle interactions as well as to more fat immobilization.

Conclusions

It can be concluded that grinding of sucrose particles via ball mill or roller mill can deliver comparable final PSD at the end of the grinding process. The results demonstrate that the particles´ surface properties are very similar at the beginning of the two grinding processes but develop in different directions during further progress in grinding. These differences in the change of particles 'surface states could be confirmed by different methods applied. The data enable a better understanding of the effect of the different grinding mechanism in the roller gap and in the ball mill. However, further research seems advisable to investigate the assumed differences in the structure of the amorphous surface state of the sucrose particles after the grinding processes.

Especially the results for roller mill grinding can be considered as highly relevant for the chocolate industry because breaking kinetics are fully comparable to those in industrial installations due to the same roller geometry and grinding kinetics. Furthermore, results can be extended to other grinding processes where crystalline particles are broken within a non-polar environment.

Author contributions Knut Franke developed software, did formal analysis and visualization of data, and wrote and edited manuscript. Ute Bindrich supervised the methodology, analyzed and validated the results as well as supervised the research project. Sarah Schroeder was involved in development of methodology and investigation, formal analysis of data, and manuscript editing. Volker Heinz was mainly responsible for acquisition of funding and project administration as well as for providing of research resources and final manuscript editing. Dana Middendorf was active in funding acquisition, developed methodology, curated and visualized data, and wrote and edited the manuscript.

Declarations

Conflict of interest The authors have no relevant financial or non-financial interests to disclose. They have no competing interests to declare that are relevant to the content of this article. All authors certify that they have no affiliations with or involvement in any organization or entity with any financial interest or non-financial interest in the subject matter or materials discussed in this manuscript. The authors have no financial or proprietary interests in any material discussed in this article.

Compliance with ethics requirements This study does not contain any experiments with human participants or animals performed by any of the authors of this paper.

References

1. Afoakwa EO (2010) Chocolate science and technology. John Wiley & Sons, Chichester
2. Ziegler GR, Hogg R (2017) Particle size reduction. In: Beckett ST, Fowler MS, Ziegler GR (eds) Beckett's industrial chocolate manufacture and use. Wiley, Chichester, pp 216–240
3. Beckett ST (2001) Milling, mixing and tempering: an engineering view of chocolate. Proc Inst Mech Eng Part E J Process Mech Eng 215:1–8. https://doi.org/10.1243/0954408011530235
4. Konar N, Bingol I (2019) Effect of ball-mill process on some quality parameters of chocolate and compound chocolate: a modeling approach. J Food Proc Engng 42:e13154. https://doi.org/10.1111/jfpe.13154
5. Rohm H, Böhme B, Skorka J (2018) The impact of grinding intensity on particle properties and rheology of dark chocolate. Food Sci Technol 92:564–568. https://doi.org/10.1016/j.lwt.2018.03.006
6. Middendorf D, Bindrich U, Mischnick P, Franke K, Heinz V (2018) AFM-based local thermal analysis is a suitable tool to characterize the impact of different grinding techniques on sucrose surface properties. J Food Eng 235:50–58. https://doi.org/10.1016/j.jfoodeng.2018.04.021
7. Windhab EJ (2000) Fluid immobilization - a structure-related key mechanism for the viscous flow behavior of concentrated suspension systems. Appl Rheol 10:134–140. https://doi.org/10.3933/ApplRheol-10-134
8. Boldyrev VV, Pavlov SV, Goldberg EL (1996) Interrelation between fine grinding and mechanical activation. Int J Miner Process 44:181–185. https://doi.org/10.1016/0301-7516(95)00028-3
9. Guckenbiehl Y, Ortner E, Rothkopf I, Schweiggert-Weisz U, Ziegleder G, Buettner A, Naumann-Gola S (2024) Distribution and transition of aroma-active compounds in dark chocolate model systems under conching conditions. Food Chem 437:137861. https://doi.org/10.1016/j.foodchem.2023.137861
10. Gloria H, Sievert D (2001) Changes in the physical state of sucrose during dark chocolate processing. J Agric Food Chem 49:2433–2436. https://doi.org/10.1021/jf0008240
11. Franke K, Heinzelmann K (2008) Structure improvement of milk powder for chocolate processing. Int Dairy J 18:928–931. https://doi.org/10.1016/j.idairyj.2008.03.013
12. Lehto VP, Tenho M, Vähä-Heikkilä K, Harjunen P, Päällysaho M, Välisaari J, Niemelä P, Järvinen K (2006) The comparison of seven different methods to quantify the amorphous content of spray dried lactose. Powder Technol 167:85–93. https://doi.org/10.1016/j.powtec.2006.05.019

13. Carstensen JT, Van Scoik K (1990) Amorphous-to-crystalline transformation of sucrose. Pharm Res 7:1278–1281. https://doi.org/10.1023/A%3A1015942022789

14. Khajehesamedini A, Paggios K, Schmid P, Kindlein M, Briesen H (2021) A population balance model for the chocolate roller refining process. Adv Powder Technol 32:4130–4140. https://doi.org/10.1016/j.apt.2021.09.021

15. Middendorf D, Bindrich U, Mischnick P, Juadjur A, Franke K, Heinz V (2016) Atomic Force Microscopy study on the effect of different lecithins in cocoa-butter based suspensions. Colloids Surf, A 499:60–68. https://doi.org/10.1016/j.colsurfa.2016.03.057

16. Lübbe J, Temmen M, Rahe P, Kühnle A, Reichling M (2013) Determining cantilever stiffness from thermal noise. Beilstein J Nanotechnol 4:227–233. https://doi.org/10.3762/bjnano.4.23

17. Falk M, Marohn F, Tewes B (2002) Foundations of statistical analyses and applications with SAS. Springer, Basel

18. Fischinger TJ, Laher M, Hild S (2014) An evaluation of local thermal analysis of polymers on the sub-micrometer scale using heated scanning probe microscopy cantilevers. J Phys Chem B 118:5570–5576. https://doi.org/10.1021/jp4092859

19. Ergun R, Lietha R, Hartel RW (2010) Moisture and shelf life in sugar confections. Crit Rev Food Sci Nutr 50:162–192. https://doi.org/10.1080/10408390802248833

20. Reiser P, Birch GG, Mathlouthi M (1995) Physical properties. In: Mathlouthi M, Reiser P (eds) Sucrose: properties and applications. Springer, Dordrecht, pp 186–222. https://doi.org/10.1007/978-1-4615-2676-6_8

21. Ziegleder G, Amanitis A, Hornik H (2004) Thickening of molten white chocolates during storage. Food Sci Technol 37:649–656. https://doi.org/10.1016/j.lwt.2004.02.003

22. IOCCC (2000) Viscosity of cocoa and chocolate products, Analytical method 46–2000. International Office of Cocoa, Chocolate and Confectionary, Brussels

23. Tscheuschner HD (1994) Rheological and processing properties of fluid chocolate. Appl Rheol 4:83–88. https://doi.org/10.2478/arh-1994-040207

24. Tüzün MA, Loveday BK, Hinde AL (1995) Effect of pin tip velocity, ball density and ball size on grinding kinetics in a stirred ball mill. Int J Miner Process 43:179–191. https://doi.org/10.1016/0301-7516(95)00009-3

25. Afoakwa EO, Paterson A, Fowler M, Vieira J (2009) Microstructure and mechanical properties related to particle size distribution and composition in dark chocolate. Int J Food Sci Technol 44:111–119. https://doi.org/10.1111/j.1365-2621.2007.01677.x

26. Afoakwa EO, Paterson A, Fowler M (2008) Effects of particle size distribution and composition on rheological properties of dark chocolate. Eur Food Res Technol 226:1259–1268. https://doi.org/10.1007/s00217-007-0652-6

27. Servais C, Jones R, Roberts I (2002) The influence of particle size distribution on the processing of food. J Food Eng 51:201–208. https://doi.org/10.1016/S0260-8774(01)00056-5

28. Marangoni AG, Rogers MA (2003) Structural basis for the yield stress in plastic disperse systems. Appl Phys Lett 82:3239–3241. https://doi.org/10.1063/1.1576502